# Shear Strength and Drift Capacity of Fiber-Reinforced Concrete Slab-Column Connections Subjected to Biaxial Displacements

Min-Yuan Cheng[1]; Gustavo J. Parra-Montesinos, A.M.ASCE[2]; and Carol K. Shield, M.ASCE[3]

**Abstract:** Results from the tests of three large-scale slab-column subassemblies subjected to combined gravity load and biaxial lateral displacements are presented. The main purpose of the experimental program was to investigate the use of randomly oriented steel fiber reinforcement as a means to increase connection punching shear strength and deformation capacity. The connection of Specimen SB1 was reinforced with regular strength (1,100 MPa) fibers, 30 mm long and 0.55 mm in diameter, while the connection of Specimen SB2 featured high-strength (2,300 MPa) fibers, 30 mm long and 0.38 mm in diameter. Both types of fibers were targeted at a 1.5% volume fraction. The connection of Specimen SB3, on the other hand, was reinforced with shear studs, designed according to the 2008 American Concrete Institute Building Code. All three connections were subjected to a gravity shear ratio of approximately 1/2 during application of biaxial lateral displacements. The use of fiber reinforcement in the connection region resulted in superior deformation capacity compared to the connection with shear stud reinforcement. Average connection rotation, just before punching, was approximately 0.04 rad in the two fiber-reinforced concrete connections. On the other hand, shear stud reinforcement seems to have had little effect on connection ductility. The connection with shear stud reinforcement failed at an average rotation of 0.023 rad. Inspection of this connection after the test indicated a breakout failure of the concrete engaged by the second line of studs accompanied by severe bending of the bottom steel rail.

**DOI:** 10.1061/(ASCE)ST.1943-541X.0000213

**CE Database subject headings:** Drift; Ductility; Studs; Plates; Fibers; Concrete slabs; Displacement; Standards and codes.

**Author keywords:** Punching shear; Drift; Ductility; Shear studs; Flat plate; Steel fibers.

## Introduction

Slab-column or flat-plate framed systems are often used in reinforced concrete construction due to economical and architectural considerations. Because the slabs are directly supported by columns, a uniform slab bottom surface is achieved, which requires simple formwork and leads to greater clear story heights. The lack of beams, however, makes the connections in these systems susceptible to punching shear failure.

Even though slab-column framed systems do not typically possess adequate lateral stiffness and strength to be relied on for earthquake resistance, they are commonly found in regions of high seismicity in combination with structural walls or special moment resisting frames. Experimental research (Pan and Moehle 1988) and postearthquake observations (Moehle 1996; Hueste and Wight 1997), however, have provided clear evidence that even when not considered to be part of the lateral load resisting system, slab-column connections are susceptible to punching shear failure under the action of earthquake-induced deformations.

[1]Design Engineer, Cary Kopczynski & Co, Bellevue, WA 98004.

[2]Associate Professor, Dept. of Civil and Environmental Engineering, Univ. of Michigan, Ann Arbor, MI 48109 (corresponding author).

[3]Professor, Dept. of Civil Engineering, Univ. of Minnesota, Minneapolis, MN 55455.

Note. This manuscript was submitted on April 8, 2009; approved on February 24, 2010; published online on February 26, 2010. Discussion period open until February 1, 2011; separate discussions must be submitted for individual papers. This paper is part of the ***Journal of Structural Engineering***, Vol. 136, No. 9, September 1, 2010. ©ASCE, ISSN 0733-9445/2010/9-1078–1088/$25.00.

The drift capacity of slab-column connections subjected to earthquake motions has been found to be strongly correlated with the intensity of connection shear stress due to gravity loads. This gravity shear stress intensity is typically expressed as the ratio of connection gravity shear stress and shear strength and is referred to as the gravity shear ratio. Fig. 1 shows a plot of drift capacity versus gravity shear ratio obtained from tests of interior connections without shear reinforcement reported in the literature (Durrani and Du 1992; Hawkins et al. 1974; Islam and Park 1976; Pan and Moehle 1988; Robertson and Durrani 1990; Robertson and Johnson 2006; Robertson et al. 2002; Symonds et al. 1976; Wey and Durrani 1990; Zee and Moehle 1984), along with the relationship adopted in the 2008 American Concrete Institute (ACI) Building Code (ACI Committee 318 2008). This relationship is used to determine, based on the design drift and gravity shear ratio, whether shear reinforcement is needed in the connection.

The use of the relationship shown in Fig. 1 between design drift and gravity shear ratio often leads to the use of shear reinforcement in slab-column connections that may be subjected to inelastic deformations induced by earthquakes. Although several types of shear reinforcements have been evaluated (e.g., bent-up bars, shearheads, hoops), headed shear stud reinforcement (Dilger and Ghali 1981) is currently the most widely used slab shear reinforcement in the United States. Shear stud reinforcement has been reported to be as effective as hoop reinforcement in resisting punching shear stresses while being easier to install (Robertson et al. 2002). Shear stud reinforcement, however, does have some drawbacks, particularly its cost. Furthermore, it may cause interference problems and reinforcement congestion.

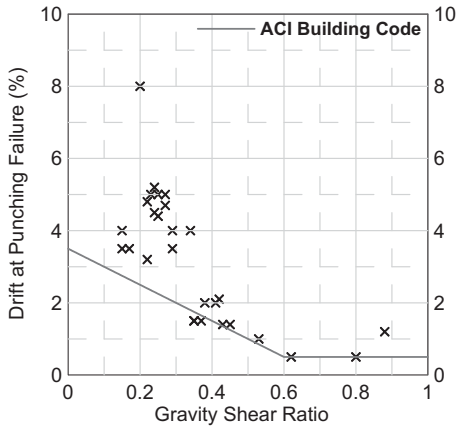


**Fig. 1.** Drift-gravity shear ratio interaction in ACI Code versus experimental data

As an economical and practical alternative to shear stud reinforcement, the use of discontinuous, randomly oriented steel fibers was investigated in this research. The tensile postcracking strength and ductility provided by fiber reinforcement in the concrete was expected to lead to an increase in connection punching shear strength and deformation capacity under combined gravity load and earthquake-induced deformations.

## Experimental Program

The seismic behavior of slab-column connections with either fiber reinforcement or headed shear studs was experimentally evaluated. Three nearly full-scale specimens, representing a first-story interior slab-column connection, were tested under combined gravity load and biaxial lateral displacement reversals at the University of Minnesota Network for Earthquake Engineering Simulation-Multi-Axial Subassemblage Testing Laboratory. These specimens are identified as SB1, SB2, and SB3. The application of biaxial lateral displacements was based on the fact that connections in service are likely to be subjected to rotations about the two principal axes during an earthquake, which has been found in laboratory experiments to lead to lower drift capacities compared to those in connections subjected to uniaxial rotations (Pan and Moehle 1988). The three test specimens were subjected to simulated gravity load to induce a connection gravity shear ratio of 1/2 [average shear stress of $(1/6)\sqrt{f'_c}$ (MPa) or $2\sqrt{f'_c}$ (psi) at the connection critical section], where $f'_c$=concrete compressive strength.

### *Specimen Geometry and Test Setup*

Plan and elevation views of the test specimens are shown in Fig. 2. Inflection points were assumed to be located at midspan of the slab in each principal direction and at midheight of the column, above the slab level. Slab dimensions were $5.18\times5.18\times0.15$ m ($204\times204\times6$ in.). The slab was supported by a 0.41 m (16 in.) square column at its center and four vertical actuators at each corner, spaced at 4.57 m (181 in.). These four vertical actuators restrained vertical displacement and twisting, while allowing biaxial lateral displacements and rotations. Eight boundary tubes served as stiffening elements along the four edges of the slab. The center column, which had a first-story length of 3.28 m or 129 in. (top of foundation to top of slab), was monolithically

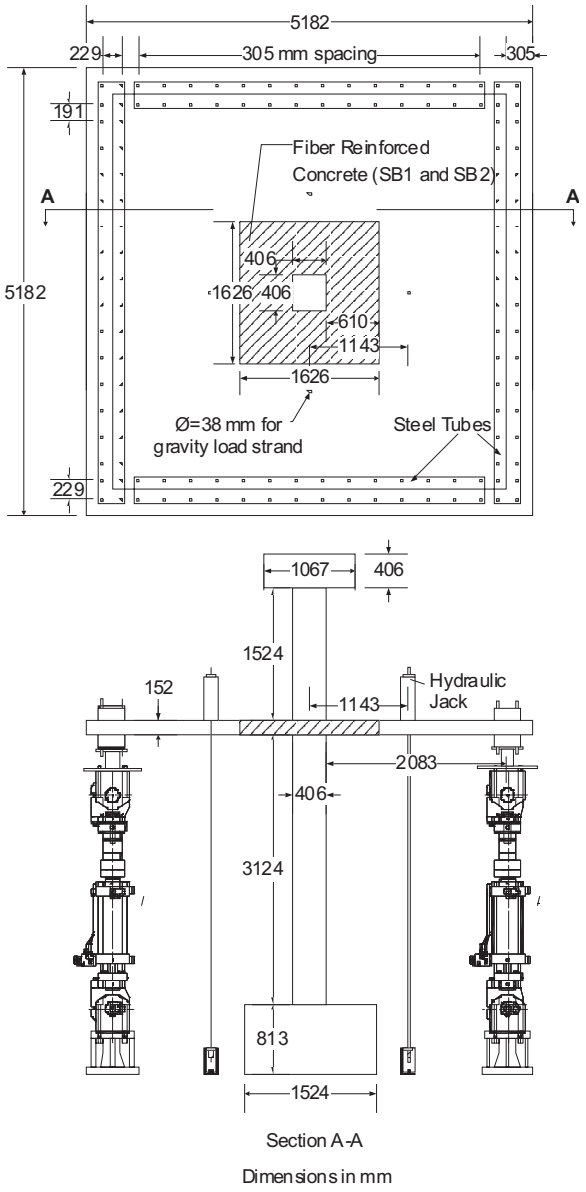


**Fig. 2.** Geometry of test specimens

connected to a heavily reinforced concrete base block which was anchored into the laboratory strong floor simulating a fixed connection. Lateral displacements were applied at the top of the column (1.93 m or 76 in. above top of the slab) through a steel crosshead. The steel crosshead, rigid for practical purposes, was driven by eight actuators and operated under a six degree-of-freedom control system. Details of the test specimens can be found elsewhere (Cheng and Parra-Montesinos 2009).

In Specimens SB1 and SB2, the 1.63 m (64 in.) square central region of the slab, defined by lines parallel to the column faces at a distance of four slab thicknesses from the face of the column, was reinforced with either regular strength (1,100 MPa) or high-strength (2,300 MPa) hooked steel fibers in a target volume fraction of 1.5% (Fig. 2). Regular concrete was used in the outer portions of the slab, as well as the other specimen components (i.e., column and base and top blocks). For Specimen SB3, reinforced by headed shear studs in the connection region, regular concrete was used throughout. A summary of the main features of the three test specimens is provided in Table 1.

**Table 1.** Main Features of Test Specimens

| Specimen | Slab dimensions: Length (m) | Slab dimensions: $h$ (mm) | Slab dimensions: $d$ (mm) | Connection shear reinforcement | Slab reinforcement: Column strip $\rho_{top}$ (%) | Slab reinforcement: Column strip $\rho_{bot}$ (%) | Slab reinforcement: Effective width[a] $\rho_{top}$ (%) | Slab reinforcement: Effective width[a] $\rho_{bot}$ (%) |
|---|---|---|---|---|---|---|---|---|
| SB1 | 5.2 | 152 | 121 | Normal strength fibers ($V_f$=1.5%) | 0.56 | 0.30 | 0.59 | 0.29 |
| SB2 | | | | High-strength fibers ($V_f$=1.36%) | | | | |
| SB3 | | | | Studs (eight rails; $d_s$=10; $s$=89) | | | | |

Note: $h$=slab thickness; $d$=slab effective depth; $V_f$=fiber volume fraction; $d_s$=shear stud diameter (mm); $s$=shear stud spacing (mm); ρ=reinforcement ratio; 1 mm=0.0394 in.; 1 m=39.4 in.; and 1 MPa=0.145 ksi.

[a]Effective width=column width+3 (slab thickness).

### Slab Flexural Reinforcement

The slab in the test specimens was designed for flexure according to the provisions in the ACI Building Code ( ACI Committee 318 2008), including continuous bottom reinforcement through the column. The flexural design procedure used resulted in a realistic ratio between the flexural strength of the slab and the demand associated with the acting gravity load, which was selected to produce a shear force corresponding to a $(1/6)\sqrt{f'_c}$ (MPa) [$2\sqrt{f'_c}$ (psi)] average shear stress (gravity shear ratio of 1/2) at the connection critical section ($d/2$ from the column face). The average slab effective depth, $d$, was 121 mm (4.75 in.). For design purposes, the concrete compressive strength and the yield strength of the reinforcement were assumed to be 34.5 MPa (5,000 psi) and 414 MPa (60 ksi), respectively. The resulting slab flexural reinforcement layout for Specimens SB1 and SB2 is shown in Fig. 3. Flexural reinforcement for Specimen SB3 had the same layout as for Specimens SB1 and SB2, except for some minor changes in the location of the bottom reinforcement within the column in order to accommodate the headed shear stud reinforcement. A detailed description of the procedure used to design the slabs can be found elsewhere (Cheng and Parra-Montesinos 2009).

The slab tension reinforcement ratio within the column strip and slab effective width (column width plus three slab thicknesses) was approximately 0.6% (Table 1). It is worth mentioning that a recent study by Widianto and Jirsa (2009) has shown that slabs with flexural reinforcement ratios in the column strip less than 1% and without shear reinforcement are susceptible to punching shear failures at substantially lower shear forces than those observed in flexurally overdesigned slabs. Even though the slab reinforcement ratio in the specimen slabs was low, it was the result of the implementation of current ACI Code provisions (ACI Committee 318 2008) and included the use of the appropriate load combinations for gravity load design and evaluation of gravity shear ratio.

### Slab Shear Reinforcement

Shear reinforcement in the connection of Specimens SB1 and SB2 consisted of randomly oriented steel fibers in a 1.5% target volume fraction. As mentioned earlier, this reinforcement was used in the connection region up to a distance of four slab thicknesses from each column face, location at which combined shear

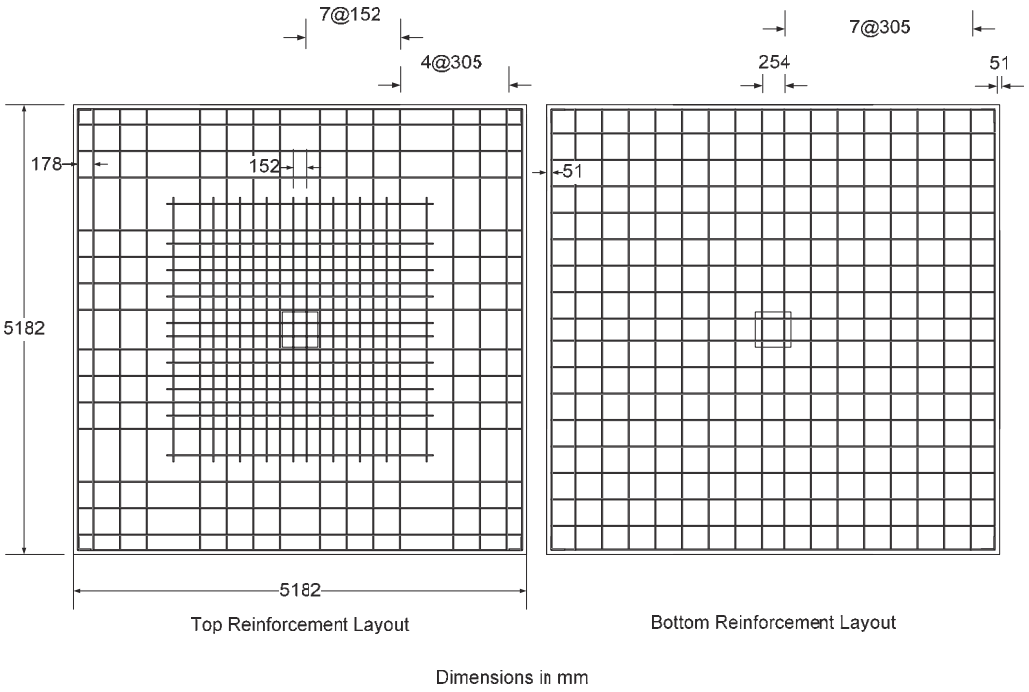


**Fig. 3.** Slab reinforcement layout

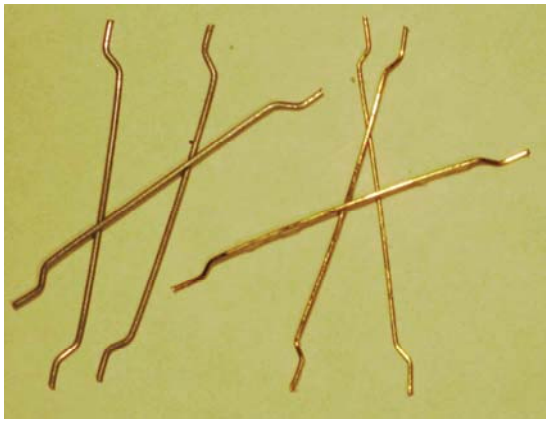

**Fig. 4.** Steel fibers used in this investigation (left: Specimen SB1; right: Specimen SB2)

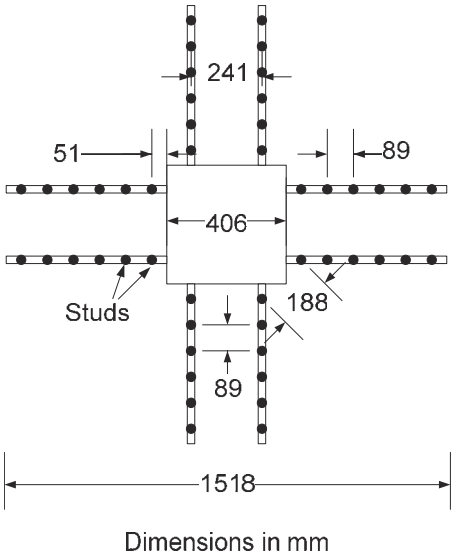


**Fig. 5.** Shear stud layout in Specimen SB3

stresses due to direct shear and unbalanced moment were expected to be less than $(1/6)\sqrt{f'_c}$ (MPa) $[2\sqrt{f'_c}$ (psi)]. Steel fibers used in Specimen SB1 were 30 mm (1.2 in.) long and 0.55 mm (0.02 in.) in diameter, and were made of a wire with a 1,100 MPa (160 ksi) tensile strength. The fibers used in Specimen SB2, on the other hand, were 30 mm (1.2 in.) long and 0.38 mm (0.015 in.) in diameter, and were made of a high-strength wire with a 2300 MPa (334 ksi) tensile strength. Fig. 4 shows a photo of the fibers used in Specimens SB1 and SB2.

The design shear stresses for the connection of Specimen SB3 were determined based on the results from the tests of Specimens SB1 and SB2. The experimental results for these two specimens indicated that for a lateral drift of 2% in either loading direction, an unbalanced moment of 170 kN·m (1,500 kip·in.) was a conservative design assumption. With this unbalanced moment, the maximum combined shear stress due to direct gravity shear and unbalanced moment at the critical section would be equal to $(0.42)\sqrt{f'_c}$ (MPa) $[5.1\sqrt{f'_c}$ (psi)]. Therefore, an 89 mm (3.5 in.) or $(3/4)d$ stud spacing was selected, which satisfies the maximum spacing requirement in the 2008 ACI Building Code (ACI 318 2008).

Eight 10 mm (3/8 in.) diameter rods were required to provide sufficient shear capacity on each peripheral line of studs, with the first rod placed 51 mm (2 in.) away from the column face. Each stud was 108 mm (4.25 in.) long, supported at the bottom by a 4.8 mm (3/16 in.) thick rail and terminated at the top with a 30 mm (1.19 in.) diameter head. As shown in Fig. 5, two stud rails, perpendicular to each column face and spaced at $2d$ (241 mm or 9.5 in.), were provided. The distance between the first stud in adjacent perpendicular rails was 188 mm (7.4 in.), which is less than $2d$. The farthest stud in each rail was located at 495 mm (19.5 in.) away from the column face. The combined shear stress due to gravity load and unbalance moment a distance $d/2$ beyond the termination of the shear reinforcement was less than $(1/6)\sqrt{f'_c}$ (MPa) $[2\sqrt{f'_c}$ (psi)].

### Column Design

The column was designed to remain elastic under the expected axial load and bending moments, except at its base. The resulting column longitudinal reinforcement consisted of 12 No. 19M (No. 6) Grade 420M (60) continuous bars with 90° hooks at both ends. Transverse reinforcement was provided at 76 mm (3 in.) spacing and consisted of four legged No. 10M (No. 3) Grade 420M (60) closed hoops.

### Application of Gravity Load

Gravity load, in addition to the slab self-weight, was simulated by four prestressing strands pulling down on the slab. The location of the strands is shown in Fig. 2. Gravity shear was calculated based on the load readings in the four vertical actuators supporting the slab corners, the slab self-weight, and the vertical load applied through the prestressing strands. The force carried by each prestressing strand was determined by the average reading of three strain gauges attached to wires in the prestressing strand whose load-strain coefficients had been determined experimentally prior to the tests. Using the slab concrete compressive strength in the connection region, the target gravity load, including slab self-weight, was determined to induce a connection gravity shear stress of $(1/6)\sqrt{f'_c}$ (MPa) $[2\sqrt{f'_c}$ (psi)]. Adjustment of the prestressing load was only made between each displacement cycle, if necessary.

### Loading Protocol

Prior to the application of lateral displacements, the column axial load and slab gravity loads were applied. The column axial load, approximately 620 kN (140 kips), was applied first and this load was held throughout the test. This load translated into an average stress, based on the gross area of the column, of approximately 10% of the concrete compressive strength. Vertical displacements at the slab corners were free to occur during application of the column axial load, but fully restrained under the application of the simulated gravity load. Each specimen was tested under the same lateral displacement history. Each displacement cycle followed a 13-step clover-leaf pattern (Fig. 6), which was the same as that used by Pan and Moehle (1988) on regular concrete connections without shear reinforcement. The use of the same clover-leaf pattern allowed a better comparison of the behavior of slab-column connections with either fiber or shear stud reinforcement with that of regular concrete connections under biaxial lateral displace-

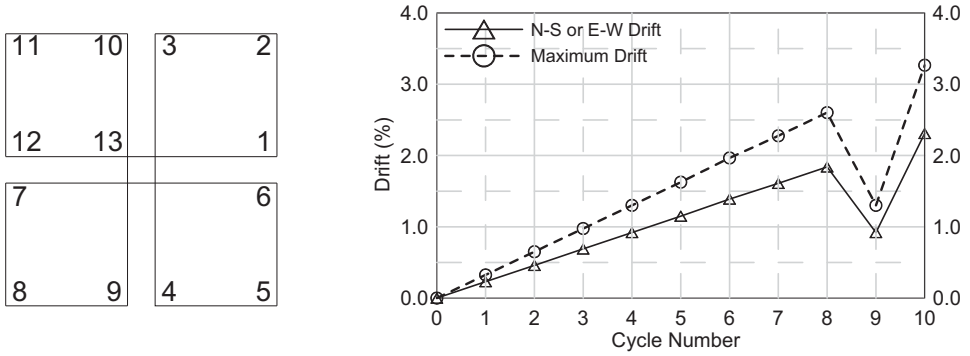


**a) Bi-axial Displacement History per Cycle**

**b) Peak Drift History**

**Fig. 6.** Lateral displacement history

ments. The tests were terminated at the end of the cycle in which a significant drop in the applied slab gravity load occurred due to punching shear failure of the connection.

## Material Properties

### *Fiber-Reinforced Concrete and Regular Concrete*

All concrete mixtures were delivered by ready-mix trucks from the same concrete supplier. The concrete for all of the specimens had the following proportions: 2.25:1.85:1:0.45 (sand: course aggregate: cement: water). Course aggregate consisted of river rock with a 10 mm (3/8 in.) maximum size.

For the slabs of Specimens SB1 and SB2, fiber-reinforced concrete was cast in the 1.63 m (64 in.) square central region, as described earlier. Fibers were mixed in the truck with the regular concrete for 3 min before casting. The remainder of the slab was cast using regular concrete from a separate ready-mix concrete truck. It should be mentioned that the volume ratio of high-strength hooked steel fibers in Specimen SB2 was 1.34%, approximately 10% less than the target volume fraction of 1.5%, because the amount of concrete delivered was greater than the volume ordered.

Concrete slump was measured before and after the addition of fibers. Prior to the addition of steel fibers, the measured concrete slump was 159 mm (6.25 in.) and 241 mm (9.5 in.) for Specimens SB1 and SB2, respectively. After the addition of fibers, the concrete slump decreased to 152 mm (6 in.) and 203 mm (8 in.) for Specimens SB1 and SB2, respectively. Both fiber-reinforced concrete materials exhibited adequate workability during casting. After the fiber-reinforced concrete was placed, only light vibration was applied where necessary. Regular concrete, from a second ready-mix concrete truck requested to arrive 15 min after the first truck, was then cast following a spiral pattern out from the interface. Once all of the concrete was placed, the entire area was vibrated as needed. The compressive strength of the concrete used in the slab for each specimen was evaluated through compressive tests of six $102\times203$ mm ($4\times8$ in.) cylinders. Even though the same mix proportions were specified, the strength of the regular concrete was higher than that of the fiber-reinforced concrete, particularly in Specimen SB2, where a 51 mm (2 in.) higher slump was measured for the concrete used in the connection (prior to adding the fibers) compared to the concrete used in the outer slab regions. Results from cylinder tests at the time of testing are summarized in Table 2.

The flexural behavior of each type of fiber-reinforced concrete was evaluated through three $152\times152\times610$ mm ($6\times6\times24$ in.) beam tests. All beams were tested under third-point loading with a 457 mm (18 in.) span length according to ASTM 1609-05 (ASTM 2005). Average results from these tests are summarized in Table 3. Both fiber-reinforced concrete materials exhibited deflection-hardening behavior. This deflection-hardening behavior was more pronounced in the fiber-reinforced concrete used in Specimen SB2 with high-strength hooked fibers, where the average residual strength at the end of the test (midspan de-

**Table 2.** Material Properties

| | Slab concrete | | Slab steel (#13M bars) | |
|---|---|---|---|---|
| Specimen | Type | Strength (MPa) | Yield strength (MPa) | Ultimate strength (MPa) |
| SB1 | Fiber reinforced | 36.9 | 424 | 659 |
| | Plain | 43.6 | | |
| SB2 | Fiber reinforced | 30.8 | | |
| | Plain | 50.9 | | |
| SB3 | Plain | 44.4 | 451 | 730 |

Note: 1 MPa=0.145 ksi.

**Table 3.** Results from ASTM 1609-05 Flexural Tests of Fiber-Reinforced Concrete Beams

| | First peak | | Second peak | | | |
|---|---|---|---|---|---|---|
| Specimen | Load (kN) | Deflection (mm) | Load (kN) | Deflection (mm) | P150,0.75 (kN) | P150,3.0 (kN) |
| SB1 | 48.6 | 0.088 | 49.4 | 0.52 | 48.0 | 35.1 |
| SB2 | 35.8 | 0.071 | 42.3 | 2.02 | 37.8 | 39.6 |

Note: P150,0.75=residual load at 0.75-mm midspan deflection for a beam with 150-mm cross-section dimension; P150,3.0=residual load at 3-mm midspan deflection for a beam with 150-mm cross-section dimension.

flection equal to 1/150 of span length) was 10% greater than the first peak (cracking) load. For the fiber-reinforced concrete used in Specimen SB1, the average residual strength at the end of the test was 25% lower than the first peak load.

### *Reinforcing Steel*

All steel reinforcing bars had a nominal yield strength of 414 MPa (60 ksi). The headed shear studs had a specified minimum yield strength of 345 MPa (50 ksi). The reinforcing steel used for Specimens SB1 and SB2 was ordered and shipped together, while the steel used in Specimen SB3 was ordered separately after the test of Specimen SB2. The measured yield and ultimate strengths for the slab reinforcement used in all three specimens are summarized in Table 2.

## Experimental Results

### *Damage Progression and Failure Mode*

Unless indicated otherwise, drift levels correspond to each principal direction [either north-south (N-S) or east-west (E-W)]. Flexural cracks on the top surface of the slabs adjacent to the column faces were observed during the 0.25 and 0.45% drift cycles. In Specimen SB3, with regular concrete, cracks on the top slab surface propagating from the corner of the column toward the corners of the slab were also observed during the cycle at 0.45% drift. In the two fiber-reinforced concrete specimens (SB1 and SB2), these cracks were observed at later stages, during the cycles between 0.9 and 1.4% drift.

When cycled to 1.15% drift, the connection of Specimen SB3 failed in punching shear, which led to the termination of the test. At this drift level, damage in the two fiber-reinforced concrete connections was negligible. At 1.6% drift, spalling of the concrete cover at the column base of Specimens SB1 and SB2 was observed, while damage in the connection region was still negligible. Punching shear-related damage in the fiber-reinforced concrete connection of Specimen SB2 was first noticed during the cycle at 1.85% drift and by the end of the 2.3% drift cycle, a full punching shear failure around the column had developed. The connection of Specimen SB1, on the other hand, showed first signs of punching shear distress during the cycle at 2.3% drift. Punching shear damage all around the column and thus, complete connection failure, became evident when this specimen was displaced to 2.75% drift.

The substantially larger drift capacity of Specimens SB1 and SB2 compared to Specimen SB3 was attributed to the ability of fibers to: (1) transfer tension across cracks once they formed and (2) control the opening of cracks, which in turn increased aggregate interlock. Unfortunately, measurements of crack width could not be made throughout the test because of safety concerns. As mentioned earlier, however, it was clear that the fiber-reinforced concrete connections exhibited significantly higher damage tolerance than the regular concrete connection.

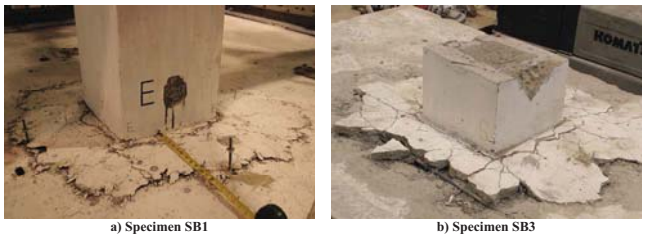


**Fig. 7.** Punching shear surface in Specimens SB1 and SB3

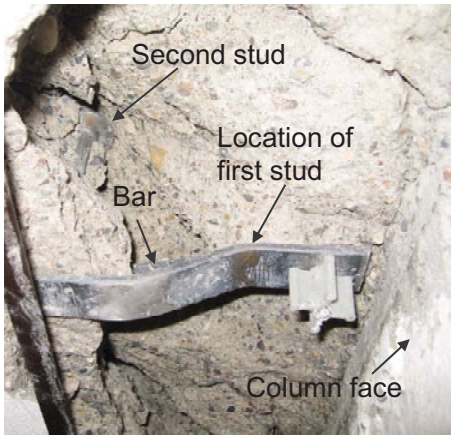


**Fig. 8.** Punching shear failure and stud reinforcement damage in Specimen SB3

The size of the punching shear surface was relatively similar for all three specimens, regardless of whether fiber reinforcement or headed shear studs were used. On average, the failure surface on the top of the slab was located 1.5 slab thicknesses away from the column faces. Figs. 7(a and b) show the punching shear surface for Specimens SB1 and SB3, respectively. The punching failure mechanism in Specimens SB1 and SB2 was fiber pullout. On the other hand, failure in Specimen SB3, with shear stud reinforcement, seemed to have been initiated with a breakout failure of the concrete engaged by the second line of studs (Fig. 8). Once the studs were not able to bridge the critical diagonal crack, the bottom rails supporting the studs were mobilized in shear through dowel action, which led to severe bending of the rails, as shown in Fig. 8.

### *Load-Drift Response and Gravity Shear History*

#### Specimen SB1

The load versus drift relationship for Specimen SB1, decomposed into N-S and E-W directions, is shown in Fig. 9. Drift is defined as the ratio between applied lateral displacement and column height (5.21 m or 205 in.) In this figure, the south and east direc-

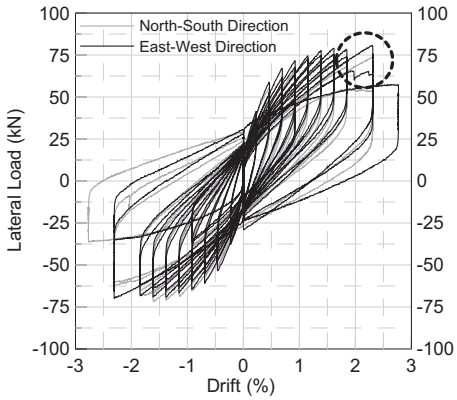


**Fig. 9.** Lateral load versus drift response (Specimen SB1)

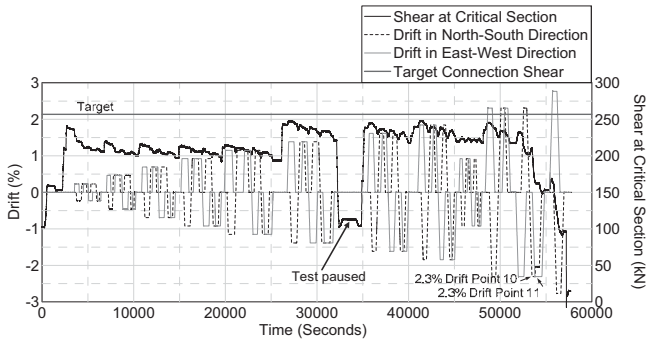


**Fig. 10.** Gravity shear history for connection of Specimen SB1

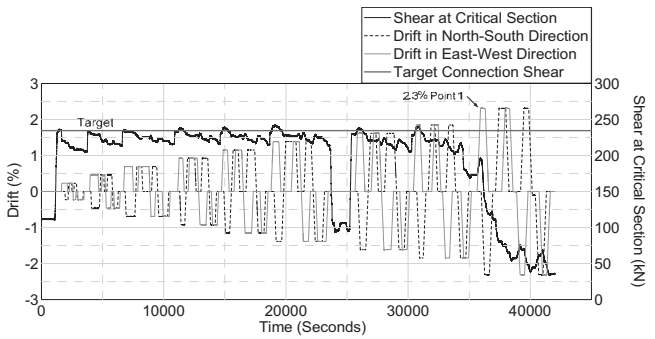


**Fig. 12.** Gravity shear history for connection of Specimen SB2

tions are defined as positive. This sign convention was applied to all test specimens. Specimen SB1 exhibited a stable hysteresis response in both loading directions throughout the cycles up to 1.85% drift. During the 2.3% drift cycle, a sudden decrease in lateral load occurred when the specimen was loaded from point 4 to point 5 in the clover-leaf loading pattern [Fig. 6(a)]; this drop is circled in Fig. 9 and was believed to have been the initiation of the punching shear failure. During the following quarter cycle at 2.3% drift, from point 6 to point 9 [Fig. 6(a)], the lateral load versus drift response did not seem to be affected by the existing damage. In the last quarter cycle at 2.3% drift, however, significant loss of lateral load resistance was observed when the specimen was loaded in the west direction (point 10 to point 11), accompanied by a significant drop in applied gravity shear. The specimen was then cycled at 2.75% drift without adjusting the applied gravity load. The test was terminated after the first quarter cycle at this drift level, once a nearly total loss of connection gravity shear capacity occurred.

The fluctuation of connection shear with time for Specimen SB1 is plotted in Fig. 10. Drift versus time histories for loading in the N-S and E-W directions are also plotted with reference to the left vertical axis. It should be mentioned that the test of Specimen SB1 was completed in 2 days. At the end of the first day of testing, the prestressing strands were unloaded and recording of data was stopped. The data plotted in Fig. 10 indicate that punching shear failure, characterized by a significant drop in the applied gravity shear, occurred between loading points 10 and 11 during the cycle at 2.3% drift. During the quarter cycle applied at 2.75% drift, the applied gravity shear dropped to negligible levels.

**Specimen SB2**

The test of Specimen SB2 was completed in 2 days as well. The load versus drift relationship for Specimen SB2 and gravity shear history are shown in Figs. 11 and 12, respectively. During this test, a gradual decrease in load occurred when the specimen was loaded from point 10 to point 11 during the 1.85% drift cycle, as encircled in Fig. 11. This was believed to have been the initiation of the punching shear failure. A significant decrease in the applied shear occurred at the end of the 1.85% drift cycle. However, the slab was still able to sustain approximately 178 kN (40 kips) of shear [shear stress of $0.13\sqrt{f'_c}$ (MPa) or $1.52\sqrt{f'_c}$ (psi) based on measured concrete strength], which was equivalent to a gravity shear ratio of 0.38 at the critical section. Therefore, it was decided to skip the cycle at 0.9% drift, and the specimen was instead further cycled at 2.3% drift without adjustment of the applied gravity load. As the specimen was pushed to loading point 1 of the 2.3% drift cycle, the gravity shear increased to 200 kN (45 kips), which corresponded to a gravity shear ratio of 0.43. The applied gravity shear then decreased significantly between loading points 1 and 2, and the connection was considered to have completely failed in punching shear. The test was terminated at the end of the 2.3% drift cycle.

**Specimen SB3**

Contrary to the tests of Specimens SB1 and SB2, the test of Specimen SB3 was completed in 1 day. The load versus drift relationship for Specimen SB3 is shown in Fig. 13. Applied connection shear and drift ratio versus time histories are shown in Fig. 14. Specimen SB3 exhibited a stable response up to loading point 6 during the cycle at 1.15% drift. When loading to point 7, a sudden drop in the lateral load occurred, which is indicated by a

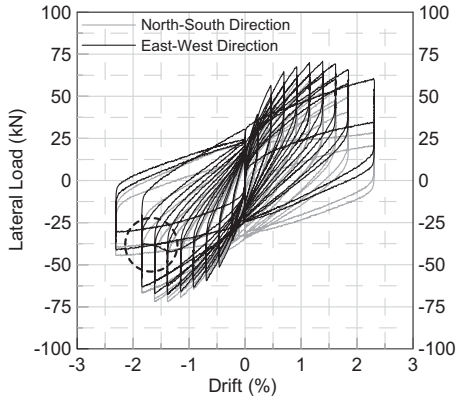


**Fig. 11.** Lateral load versus drift response (Specimen SB2)

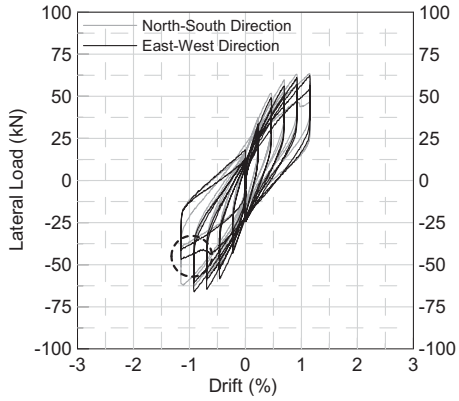


**Fig. 13.** Lateral load versus drift response (Specimen SB3)

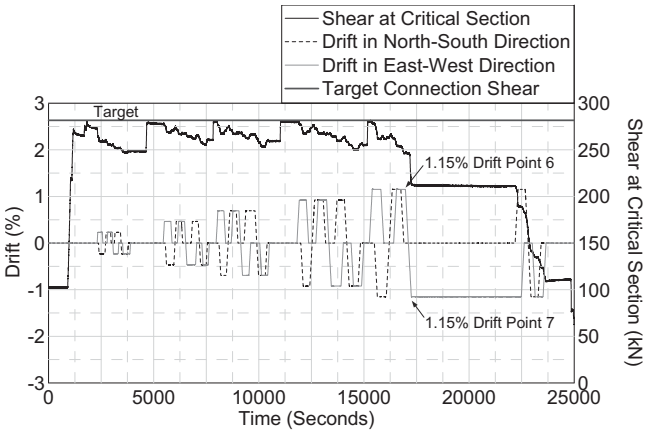


**Fig. 14.** Gravity shear history for connection of Specimen SB3

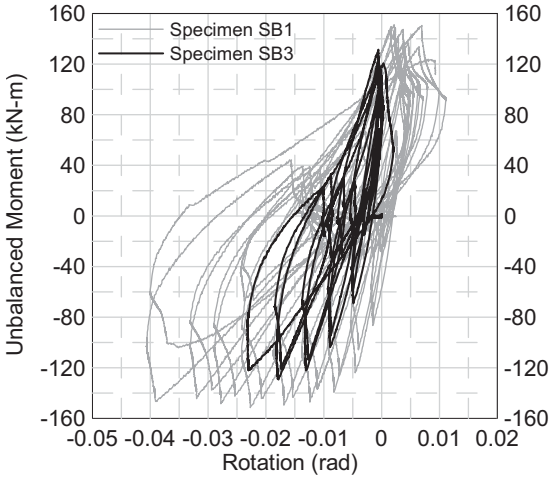


**Fig. 15.** Unbalanced moment (*N-S*) versus rotation (*N*) response (Specimens SB1 and SB3)

circle in Fig. 13. This point was believed to mark the initiation of the punching shear failure in Specimen SB3. Unlike Specimens SB1 and SB2, the lateral load resistance of Specimen SB3 decreased for both loading directions during the remaining loading steps at 1.15% drift. From Fig. 14, it can be seen that a significant drop in gravity shear occurred when the specimen was loaded from point 6 to point 7 during the 1.15% drift cycle. At the end of this cycle, an attempt to increase the applied gravity shear to the target level was unsuccessful, which led to the termination of the test.

Comparing the hysteresis behavior of all three specimens, it can be seen that prior to failure the specimens exhibited similar responses (e.g., similar strength, stiffness and energy dissipation capacity), which were dominated by the flexural behavior of the slab. Specimens SB1 and SB2, however, exhibited a slightly higher strength compared to Specimen SB3. This is attributed to the postcracking tensile resistance of the fiber concrete, which provided a modest increase to the connection moment strength.

### Connection Rotations and Spread of Yielding

Slab rotations were measured through LVDTs at a distance of $1d$ and $2d$ from each column face. In all three test specimens, most of the connection rotations concentrated over a distance of $1d$ from each column face. Rotation values reported will thus refer to those measured at $1d$ from the column faces. Fig. 15 shows the unbalanced moment (N-S direction) versus slab rotation (north) response for Specimens SB1 and SB3. Negative bending implies tension at the top surface of the slab. As can be seen, a rotation slightly less than 0.01 rad corresponded to first yielding of the slab in Specimen SB1, which occurred during the cycle at 0.7% drift. Maximum unbalanced moment corresponded to a rotation, on average, of approximately 0.015 rad. The peak unbalanced moment during subsequent loading cycles remained relatively constant up to a slab rotation of approximately 0.04 rad, when a punching shear failure initiated. The behavior of Specimen SB2 was similar to that of Specimen SB1, with maximum rotations at punching shear failure between 0.036 and 0.044 rad for all four connections sides.

Strain gauge data indicate that yielding of the top steel reinforcement across the slab width of Specimen SB1 was limited to the bars located within the central 760 mm (30 in.) of the slab, which corresponded approximately to a width of $C_2+3d$, where $C_2$=column width. For the slab of Specimen SB2, on the other hand, yielding of flexural reinforcement was limited to a width of 610 mm (24 in.), which is approximately equal to a width of $C_2+2d$. Along the direction of the slab bars, reinforcement yielding was rather localized, as indicated by strain gauge readings and the fact that most of the connection rotations occurred within a distance of $1d$ from the column faces.

The behavior of Specimen SB3 with headed shear studs was characterized by a limited connection rotation capacity, as shown in Fig. 15. Maximum rotation at failure on all four sides of the connection ranged between 0.02 and 0.027 rad. As in Specimen SB1, slab flexural yielding in this specimen was limited to the bars located within the central 760 mm ($C_2+3d$) region of the slab.

### Column Base Rotations

Column base rotations were measured through LVDTs over a distance of 355 mm or 14 in. (column effective depth). First yielding of the longitudinal reinforcement corresponded to a column base rotation of approximately 0.005 rad. By the end of the 2.3% drift cycle, the column base in Specimens SB1 and SB2 had undergone moderate inelastic rotations (peak total rotation on the order of 0.015 rad). For Specimen SB3, on the other hand, the peak column base rotation was approximately 0.0075 rad (1.15% drift cycle).

### Evaluation of Shear Stresses Using Eccentric Shear Model

In the two principal directions, N-S and E-W directions, the combined shear stress $v$ at the critical section of the connection due to direct shear $V$ and unbalanced moment $M_{ub}$ at each peak drift was calculated using the "eccentric shear model" specified in the ACI Building Code (ACI Committee 318 2008). In this model, which is based on the work by DiStasio and Van Buren (1960), Moe (1961), and Hanson and Hanson (1968), the combined shear stress is calculated as follows:

$$v = \frac{V}{A_c} \pm \frac{\gamma_v M_{ub} c}{J_c} \tag{1}$$

where $A_c$=area defined by the critical perimeter multiplied by the slab effective depth; $c$=distance measured from the centroid of the support to the critical perimeter; $\gamma_v M_{ub}$=fraction of unbal-

anced moment transfer through eccentric shear; and $J_c$=property "analogous to the polar moment of inertia." For the connections tested and considering the critical section to be at $d/2$ from the column face, $A_c$=0.254 m$^2$ (394.25 in.$^2$), $c$=264 mm (10.375 in.), $\gamma_v$=0.4, and $J_c$=0.0119 m$^4$ (28662 in.$^4$). Typically, combined shear stresses in slab-column connections are calculated independently for each principal direction. Eq. (1), however, can be expanded to calculate stresses due to the action of biaxial unbalanced moments. In this case, the peak shear stress would apply to a corner point in the connection critical section, as opposed to the combined shear stress for uniaxial bending, which applies to an entire side of the critical section.

Normalized shear stress values reported herein are based on measured concrete compressive strength at the day of testing. In Specimens SB1 and SB2, the peak combined shear stress for loading in each principal direction was approximately equal to $0.38\sqrt{f'_c}$ (MPa) [$4.5\sqrt{f'_c}$ (psi)]. For Specimen SB3, with shear stud reinforcement, the peak shear stress was approximately $0.33\sqrt{f'_c}$ and $0.36\sqrt{f'_c}$ (MPa) [$4\sqrt{f'_c}$ and $4.3\sqrt{f'_c}$ (psi)] for loading in the N-S and E-W direction, respectively. It should be noted that the peak shear stress in the N-S and E-W direction for Specimen SB3 is, respectively, equal to and slightly larger than the shear stress limit for which no shear reinforcement is required in slab-column connections $(1/3)\sqrt{f'_c}$ (MPa) [$4\sqrt{f'_c}$ (psi)], according to the ACI Building Code (ACI 318 2008).

When biaxial bending is considered, a peak shear stress of $0.54\sqrt{f'_c}$ and $0.58\sqrt{f'_c}$ (MPa) [$6.5\sqrt{f'_c}$ and $7.0\sqrt{f'_c}$ (psi)] is obtained for Specimens SB1 and SB2, respectively. For Specimen SB3, on the other hand, the peak shear stress caused by gravity-induced shear and biaxial bending was $0.48\sqrt{f'_c}$ (psi) [$5.7\sqrt{f'_c}$ (psi)].

In the E-W direction, the maximum shear stresses (absolute peak value) in Specimens SB1 and SB2 were 8 and 14% higher, respectively, than the peak shear stress in Specimen SB3. In the N-S direction, these stresses were 13 and 20% higher for Specimens SB1 and SB2, respectively, compared to Specimen SB3. From either the "uniaxial eccentric model" or the "biaxial eccentric model," the largest punching shear stress among all three test specimens was carried by Specimen SB2. The lower shear stress demand in Specimen SB1, combined with the 10% higher fiber content compared to Specimen SB2, could explain the slightly larger ductility exhibited by Specimen SB1.

### Evaluation of Contribution of Shear Stud Reinforcement

The nominal shear stress capacity of the connection in Specimen SB3 (based on nominal material properties), calculated according to the 2008 ACI Building Code (ACI Committee 318 2008) as the summation of the "concrete" and the shear stud contributions to shear strength, was equal to $0.43\sqrt{f'_c}$ (MPa) [$5.14\sqrt{f'_c}$ (psi)] or 2.51 MPa (364 psi). It is worth mentioning that the ACI Code allows the use of a concrete shear strength contribution of $(1/4)\sqrt{f'_c}$ (MPa) [$3\sqrt{f'_c}$ (psi)] when shear stud reinforcement is used, which is 50% greater than the allowed concrete contribution when other types of shear reinforcements are used. Because the measured concrete cylinder strength (44.4 MPa) was greater than assumed in design (35 MPa), the nominal connection shear stress capacity based on the measured concrete strength was 2.71 MPa (393 psi). The peak shear stress demand obtained using Eq. (1), however, was 2.37 MPa (345 psi), calculated at point 1 during the 0.9% drift cycle, which is 12% lower than the calculated shear stress capacity. If the concrete contribution to shear strength is reduced by 25%, as recommended by ACI-ASCE Committee 352 (1989) to account for the effect of inelastic displacement reversals, a shear stress capacity of 2.29 MPa (333 psi) would be obtained, which is just 4% below the calculated shear stress demand.

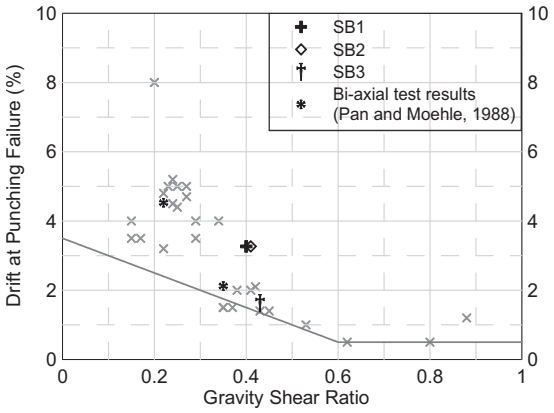


**Fig. 16.** Drift versus gravity shear ratio interaction

From inspection of the connection in Specimen SB3 after punching shear failure, it seems that the shear stud reinforcement was not effective in bridging the primary punching shear crack once it formed, as evidenced by the breakout failure of the concrete engaged by the second line of studs (Fig. 8). One argument that could be made is that shear resisted through aggregate interlock in connections with shear studs is likely to be smaller than that in connections with hoops or bent-up bars. This is because shear studs rely on mechanical anchorage at their ends with little or no bond along their length, which requires the opening of a wider diagonal crack in order for the studs to reach their yield strength. In this case, the use of $(1/4)\sqrt{f'_c}$ (MPa) [$3\sqrt{f'_c}$ (psi)] for the concrete contribution to shear strength may not be appropriate. On the other hand, the use of $(1/6)\sqrt{f'_c}$ (MPa) [$2\sqrt{f'_c}$ (psi)], as for connections with shear reinforcement other than shear studs, reduced by 25% to account for the effect of inelastic displacement reversals (ACI-ASCE Committee 352 1989), would have led to a safe prediction of the shear capacity of the connection. More troubling, however, is the fact that the shear stud reinforcement seems to have had little effect on connection ductility, especially given the fact that the peak shear stress demand was less than 10% higher than the shear stress level for which shear reinforcement is not required for the configuration tested $(1/3)\sqrt{f'_c}$ (MPa) [$4\sqrt{f'_c}$ (psi)].

### Influence of Gravity Shear Ratio on Drift Capacity

The drift versus gravity shear ratio relationship previously shown in Fig. 1 is replotted in Fig. 16, including the test results from Specimens SB1, SB2, and SB3, as well as the data corresponding to the biaxial tests on slab-column connections without shear reinforcement conducted by Pan and Moehle (1988). The resultant (total) drift ratio was used for these specimens.

From Fig. 16, it is seen that the experimental results from Specimens SB1, SB2, and SB3 were above the envelope relationship in the ACI Building Code (ACI Committee 318 2008). While the failure drifts for Specimens SB1 and SB2 are considerably greater than the drift assumed in the ACI Code relationship, the data point corresponding to Specimen SB3 is close to this relationship and comparable to several test results from connections without shear reinforcement, which were obtained from tests

under uniaxial displacement reversals. Furthermore, this data point is located at approximately the same distance from the ACI Code envelope as one of the connections without shear reinforcement tested by Pan and Moehle (1988) under biaxial loading. This suggests that shear stud reinforcement had little to no effect on the ductility of Specimen SB3. It should be mentioned that the connections tested by Pan and Moehle had a similar longitudinal reinforcement ratio within the slab effective width (0.62% versus 0.59%), but a lower reinforcement ratio within the column strip (0.44% versus 0.56%) compared to those in Specimen SB3.

## Conclusions

From the results of the tests of three nearly full-scale slab-column connections under combined gravity load and biaxial lateral displacement reversals, the following conclusions can be drawn.

- Hooked steel fibers in a 1.5% volume fraction were effective in increasing the ductility of slab-column connections subjected to combined gravity load and biaxial lateral displacement reversals. Punching shear failure of Specimens SB1 and SB2, with fiber-reinforced concrete, occurred during the cycle at 3.3% total drift (2.3% drift in each principal direction) under a gravity shear ratio of approximately 0.4. Specimen SB3, whose connection was reinforced with headed shear studs, failed in punching shear during the 1.6% drift cycle (1.15% drift in each principal direction) under approximately the same gravity shear ratio.
- Compared to the connection with headed shear stud reinforcement, the fiber-reinforced concrete specimens exhibited over 70% greater average rotation capacity. In the two fiber-reinforced concrete specimens (SB1 and SB2), average connection rotation prior to punching shear failure was approximately 0.04 rad. The average rotation at failure for Specimen SB3 with shear stud reinforcement, on the other hand, was 0.023 rad. All three test connections were subjected to approximately the same peak combined shear stress (approximately $0.38\sqrt{f'_c}$ (MPa) [$4.5\sqrt{f'_c}$ (psi)] for bending about each principal direction.
- Headed shear stud reinforcement did not seem to be effective in bridging the critical diagonal crack and thus, in increasing connection punching shear resistance and deformation capacity. Although the peak shear stress due to direct shear and unbalanced moment was only slightly greater than the upper shear stress limit for which no shear reinforcement is required according to the 2008 ACI Building Code [$(1/3)\sqrt{f'_c}$ (MPa)], punching shear failure occurred at an average rotation of 0.023 rad. Failure was characterized by a breakout failure of the concrete engaged by the second line of studs accompanied by severe bending of the rail supporting the studs. Based on these results, further experimental research on the behavior of slab-column connections with headed shear stud reinforcement under combined gravity load and lateral displacement reversals is warranted.
- Based on the limited test results and until further experimental data become available, the concrete contribution to shear strength of connections with shear stud reinforcement should be taken as $0.75(1/6)\sqrt{f'_c}$ (MPa) [$0.75\cdot 2\sqrt{f'_c}$ (psi)], as recommended by ACI Committee 352 for connections with shear reinforcement other than shear studs subjected to inelastic displacement reversals.

## Acknowledgments

This research was sponsored by the U.S. National Science Foundation, as part of the Network for Earthquake Engineering Simulation (NEES) Program, under Grant No. CMS 0421180. The opinions expressed in this paper are those of the writers and do not necessarily express the views of the sponsor.

## References

American Concrete Institute (ACI)-ASCE Committee 352. (1989). "Recommendations for design of slab-column connections in monolithic reinforced concrete structures (reapproved 2004)." *352.1R-89*, Farmington Hills, Mich., 1–26.

American Concrete Institute (ACI) Committee 318. (2008). "Building code requirements for reinforced concrete and commentary." *ACI 318-08*, Farmington Hills, Mich.

ASTM. (2005). "Standard test method for flexural performance of fiber-reinforced concrete (using beam with third-point loading)." *C1609/C 1609M-05*, West Conshohocken, Pa.

Cheng, M.-Y., and Parra-Montesinos, G. J. (2009). "Punching shear strength and deformation capacity of fiber reinforced slab-column connections under earthquake-type loading." *Rep. No. UMCEE 09-01*, Dept. of Civil and Environmental Engineering, Univ. of Michigan, Ann Arbor, Mich.

Dilger, W. H., and Ghali, A. (1981). "Shear reinforcement for concrete slabs." *J. Struct. Div.*, 107(12), 2403–2420.

Di Stasio, J., and Van Buren, M. P. (1960). "Transfer of bending moment between flat-plate floor and column." *ACI J.*, 57(9), 299–314.

Durrani, A. J., and Du, Y. (1992). "Seismic resistance of slab-column connections in existing non-ductile flat-plate buildings." *Technical Rep. No. NCEER-92-0010*, Dept. of Civil Engineering and Mechanical Engineering, Rice Univ., Houston.

Hanson, N. W., and Hanson, J. M. (1968). "Shear and moment transfer between concrete slabs and columns." *Bulletin D129*, Development Dept., Research and Development Laboratories, Portland Cement Association, 16.

Hawkins, N. M., Mitchell, D., and Sheu, M. S. (1974). "Cyclic behavior of six reinforced concrete slab-column specimens transferring moment and shear." *Progress Rep. No. 1973-74*, Dept. of Civil Engineering, Univ. of Washington, Seattle.

Hueste, M. B. D., and Wight, J. K. (1997). "Evaluation of a four-story reinforced concrete building damaged during the Northridge earthquake." *Earthquake Spectra*, 13(3), 387–414.

Islam, S., and Park, R. (1976). "Tests of slab-column connections with shear and unbalanced flexure." *J. Struct. Div.*, 102(ST3), 549–569.

Moe, J. (1961). "Shearing strength of reinforced concrete slabs and footings under concentrated loads." *Bulletin D47*, Development Dept., Research and Development Laboratories, Portland Cement Association, 130.

Moehle, J. P. (1996). "Seismic design considerations for flat-plate construction." *ACI special publication 162, Mete A. Sozen symposium: A tribute from his students*, J. K. Wright and M. E. Kreger, eds. American Concrete Institute, Farmington Hills, Mich., 1–34.

Pan, A. A., and Moehle, J. P. (1988). "Reinforced concrete flat plates under lateral loadings: an experimental study including biaxial effects." *Rep. No. UCB/EERC-88/16*, Earthquake Engineering Research Center, Univ. of California at Berkeley, Berkeley, Calif.

Robertson, I. N., and Durrani, A. J. (1990). "Seismic response of connections in indeterminate flat-slab subassemblies." *Rep. No. 41*, Rice Univ., Houston.

Robertson, I. N., and Johnson, G. (2006). "Cyclic lateral loading of non-ductile slab-column connections." *ACI Struct. J.*, 103(3), 356–364.

Robertson, I. N., Kawai, T., Lee, J., and Johnson, G. (2002). "Cyclic testing of slab-column connections with shear reinforcement." *ACI Struct. J.*, 99(5), 605–613.

Symonds, D. W., Mitchell, D., and Hawkins, N. M. (1976). "Slab-column

connections subjected to high intensity shears and transferring reversed moments." *Rep. No. SM 76-2*, Div. of Structures and Mechanics, Dept. of Civil Engineering, Univ. of Washington, Seattle.
Wey, E. H., and Durrani, A. J. (1990). "Seismic response of slab-column connections with shear capitals." *Rep. No. 42*, Rice Univ., Houston.
Widianto, Bayrak O., and Jirsa, J. O. (2009). "Two-way shear strength of slab-column connections: Reexamination of ACI 318 provisions." *ACI Struct. J.*, 106(2), 160–170.
Zee, H. L., and Moehle, J. P. (1984). "Behavior of interior and exterior flat plate connections subjected to inelastic load reversals." *Rep. No. UCB/EERC-84/07*, Earthquake Engineering Research Center, Univ. of California at Berkeley, Berkeley, Calif.